J. Mt. Sci. (2023) 20(6): 1561-1574 e-mail: jms@imde.ac.cn http://jms.imde.ac.cn
https://doi.org/10.1007/s11629-022-7707-9

Original Article

Effects of phosphorus fertilizer application rate on transformation processes of phosphorus fractions in the purple alluvial soil of a riparian zone

HE Li-ping[1] https://orcid.org/0000-0001-9438-6175; e-mail: hlp_weird@163.com

JIA Kai-tao[1] https://orcid.org/0000-0001-9274-7766; e-mail: 1580289098@qq.com

LIU Dan[2] https://orcid.org/0000-0003-0103-4475; e-mail: liudan750@126.com

WANG Ke-hong[1] https://orcid.org/0000-0001-9592-1221; e-mail: wang018837@hotmail.com

DUAN Lin-Yan[1] https://orcid.org/0009-0005-7055-8530; e-mail: 1527711486@qq.com

LIN Jun-jie[1*] https://orcid.org/0000-0003-0955-3106; e-mail: junjielin@sanxiau.edu.cn

**Corresponding author*

1 Key Laboratory of Water Environment Evolution and Pollution Control in the Three Gorges Reservoir, Chongqing Three Georges University, Chongqing 404100, China

2 Department of Agricultural and Forestry Science and Technology, Chongqing Three Gorges Vocation College, Chongqing 404000, China

Citation: He LP, Jia KT, Liu D, et al. (2023) Effects of phosphorus fertilizer application rate on transformation processes of phosphorus fractions in the purple alluvial soil of a riparian zone. Journal of Mountain Science 20(6). https://doi.org/10.1007/s11629-022-7707-9

Abstract: Effects of phosphorus (P) fertilizer application rate on soil transformation processes of P fraction are still unclear in the riparian zone. Purple alluvial soils in the riparian zone of the Three Gorges Reservoir were collected to conduct a 21-day incubation executed by two hydrological environments (drying and flooding) and ten application rates of P fertilizer. Transformation percentages of P fertilizer (TPPF) were calculated as content differences of soil P fractions between fertilizer addition and none fertilizer addition divided by soil total P increases caused by fertilizer addition. TPPF to inorganic P extracted by sodium hydroxide (NaOH-Pi) and hydrochloric acid (HCl-Pi) increase by 20.91% (9.71%) and 24.26% (40.72%) under the drying (flooding) environment. Instead, TPPF to the other fractions decrease. Phosphorus fertilizer input mainly has indirect positive and negative effects on organic P via precipitated P under the drying and flooding environments and finally has indirect positive effects on labile P (p<0.001). Percentage changes of water-soluble inorganic P (H_2O-Pi) and HCl-Pi under the flooding environment are higher than that under the drying environment, and percentage changes of organic P extracted by sodium hydrogen carbonate ($NaHCO_3$-Po) and NaOH-Pi show an opposite trend (p<0.01). Δ (differences in soil P fraction content between flooding and drying incubations) H_2O-Pi is negatively correlated with $\Delta NaHCO_3$-Po, and $\Delta NaHCO_3$-Po is positively correlated with ΔNaOH-Pi (p <0.001). In conclusion, P fertilizer is transformed more into precipitated P than into other P fractions with an application rate increase. Phosphorus fertilizer input mainly increases organic P via precipitated P under the drying environment and decreases organic P via precipitated P under the flooding environment, and organic P is

Received: 09-Sep-2022
1st Revision: 11-Dec-2022
2nd Revision: 28-Feb-2023
Accepted: 06-Apr-2023

further transformed into labile P. With P fertilizer input, P release caused by flooding is derived from $NaHCO_3$-Po release triggered by NaOH-Pi release. The results can be helpful for the understanding of P fertilizer migration processes from the riparian zone soil to the Three Gorges Reservoir under rain leaching and flooding.

Keywords: Hedley fractionation; Phosphorus fraction; Hydrological environments; Three Gorges Reservoir; Application rate; Riparian zone

1 Introduction

The riparian zone is a transition of land and aquatic ecosystems. Drying and flooding environments are the main hydrological environments in the riparian zone (Chen et al. 2019). Phosphorus (P) fertilizer input from agriculture has become an important factor for soil P release increase from the riparian zone to its surrounding water under the drying environment, resulting in eutrophication (Chen et al. 2021; Fu et al. 2021; Xiang et al. 2021).

Soil P fraction distribution as affected by applied P fertilizer determines further P release potential to surrounding water (Yan et al. 2017; Zhu et al. 2012) since different soil P fraction has different migration ability. Under P fertilizer input, there are differences in the distribution and transformation of soil P fractions between the drying and flooding environments (Wang et al. 2021). Studies have been conducted on this issue under drying and flooding environments in recent years. Under the drying environment, inorganic P fertilizer is mainly transformed into inorganic P fractions (Chen et al. 2022a; Yan et al. 2018; Cao et al. 2022; Mitran et al. 2016), leading to a decrease in organic P percentage in soil total P, while it is not clear into which inorganic P fraction inorganic P fertilizer is transformed. Inorganic P fertilizer is mainly transformed into iron(Fe)-bound P and aluminum(Al)-bound P in acidic soil (Chen et al. 2022a), whereas mainly transformed into calcium (Ca)-bound P in saline soil (Meena et al. 2018). Under the flooding environment, inorganic P fertilizer input reduces residual P content and increases Ca-bound P content in paddy soil (Ahmed et al. 2019; Huang et al. 2014). Meanwhile, it has also been found that organic P increases and adsorbed P decreases in paddy soil (Huang et al. 2014). In terms of fraction transformation mechanisms, scholars believe that inorganic P fertilizer is first transformed into labile P and precipitated P under the drying environment (Audette et al. 2016; Jiménez et al. 2019). Meanwhile, there is a controversy on the further transformation direction of P fractions. One opinion is that soil P fractions are further transformed into more stable fractions (Audette et al. 2016), and the other opinion is that soil P fractions are further transformed into more labile fractions (Jiménez et al. 2019). In summary, current studies have explored soil fraction distribution after P fertilizer application under the drying and flooding environments, and P transformation mechanisms under the drying environment. However, there are still shortcomings. Transformation mechanisms of soil P fraction as affected by applied P fertilizer are cursorily studied under the drying environment, needing further investigation, especially for mutual transformation processes between P fractions. In addition, soil P fraction distribution as affected by applied P fertilizer is rarely reported under the flooding environment, and transformation mechanisms of soil P fraction are still unclear. Moreover, related issues have been mainly investigated in acidic soil, saline soil, and paddy soil. Caused by soil property differences, P fraction distribution, and transformation mechanism are still controversial. Therefore, other soil types should be selected to clarify key factors affecting the distribution and transformation processes of P fraction affected by applied P fertilizer.

The Three Gorges Reservoir (TGR) area is located upstream of the Yangtze River, stretching from Yichang City in Hubei Province to the Jiangjin City in Chongqing. This area is characterized by a humid subtropical monsoon climate with a frontal rainfall pattern, an average annual temperature of 16°C–19°C, and average annual precipitation of 1000–2000 mm. In addition, the annual average flow of the Yangtze River is 13,200 $m^3 s^{-1}$ in the Wanzhou section, and the maximum storage capacity of the TGR is 39.3 billion m^3. The water level of the TGR is artificially controlled, dropping from 175 m in January to 145 m in July and then gradually rising to 175 m in September, forming a riparian zone with a total area of 349 km^2 after the operation of the Three Gorges Dam (Bao et al. 2015). Alternating drying and flooding processes inevitably trigger soil redox potential changes, which affects the distribution and transformation of soil P fractions in the riparian zone (Wang et al. 2021). In addition, the

land use pattern around the riparian zone is farmland and grassland, resulting in exogenous P input to the riparian zone. Scholars have carried out some studies on soil P fractions in recent years, since releasing of soil P from the riparian zone to the TGR (Ye et al. 2019; Wang et al. 2020). Calcium-bound P is the main soil P fraction of the riparian zone, followed by organic P and Al/Fe-bound P in descending order (Zhang et al. 2018). In addition, drying and flooding processes significantly increase soil contents of organic P, Ca-bound P, and residual P in the riparian zone (Wang et al. 2021). Furthermore, inorganic P fractions were found to be the main source of labile P under alternating environments of drying and flooding, which is closely related to microbial P, organic P, and amorphous Fe (Wang et al. 2021). The above studies have explored P fraction distribution and the effect of alternating drying and flooding on it in the riparian zone soil. However, the effects of P fertilizer input on P fraction distribution and transformation are still unclear in the riparian zone soil.

To investigate soil P fraction distribution and transformation mechanism as affected by applied P fertilizer under the drying and flooding environments, we collected purple alluvial soil in the riparian zone of the TGR to conduct an incubation experiment executed by two soil hydrological environments (the drying and flooding environments) and ten application rates of P fertilizer. The objects of the study were (1) to clarify P fraction distribution in the purple alluvial soil of the riparian zone as affected by applied P fertilizer under the drying and flooding environments; (2) to reveal transformation processes of soil P fractions as affected by applied P fertilizer in terms of P release. (3) to assess the effects of flooding on soil P fraction distribution and transformation after P fertilizer application. The modified Hedley sequential P fractionation procedure is a method that adopts solutions with gradually increasing extraction strength to extract soil P fraction from diverse inorganic and organic compounds of different lability (Maranguit et al. 2017b; Redel et al. 2008). This method differentiates soil P fractions into labile P, precipitated P, organic P, and residual P, which is widely accepted for assessing the release risk of soil P and exploring P cycle processes (Gu and Margenot 2021). Because of the high contents of Al and Fe oxides/hydroxides and Ca carbonate in the purple alluvial soil (Li et al. 2007) and the dominant roles of microorganisms in soil P cycle processes (Han et al. 2022; Saia et al. 2021; Zhang et al. 2021), we hypothesize that (1) P fertilizer is mainly transformed into precipitated P, and increase in P fertilizer application rate will increase transformation percentages of P fertilizer to precipitated P; (2) Precipitated P can be further transformed into organic P and labile P by microorganisms under the drying and flooding environments; (3) Flooding will result in transformation of Fe-bound P and adsorbed organic P to water-soluble P and Ca-bound P.

2 Materials and Methods

2.1 Soil sampling and pretreatment

Purple alluvial soil is a major soil type of the riparian zone of the TGR in the Wanzhou section, which is derived from sand shale, and vermiculite is the dominant clay mineral (China Soil Database, http://vdb3.soil.csdb.cn). The riparian zone is sloping land, and the land use type of which is grassland during the drying period. Soils (0–20 cm) were randomly collected from the riparian zone (N30°47.28′–30°50.10′, E108°21.35′–108°23.41′) by a soil corer with a diameter of 5 cm in June 2018 (Fig. 1). The soils were mixed and divided into two parts after freeze-drying and the removal of gravel, animal, and plant residue. One part was sieved through a 2 mm sieve and utilized for soil physicochemical property analyses including particle composition, pH, water-holding capacity (WHC), total carbon (TC), total nitrogen (TN), C: N ratio, cation exchange capacity (CEC), total P (TP, Table 1) and soil content of P fractions (Table 2). The other part was sieved through a 12 mm mesh and utilized for incubation experiments.

2.2 Soil incubation

Ten application rates of P fertilizer (0, 5, 20, 35, 50, 65, 80, 95, 140, 230 kg P ha^{-1} corresponding to 0, 11.74, 46.95, 82.16, 117.37, 152.58, 187.79, 223.00, 328.64, 539.91 mg kg^{-1}) and two hydrological environments (drying and flooding) were set with three replicates for each treatment. In total, 60 soil samples were incubated (10× 2 ×3). First, 100 g soils were evenly placed in plastic bottles (3 cm depth) with soil moisture content adjusted to 50% WHC by

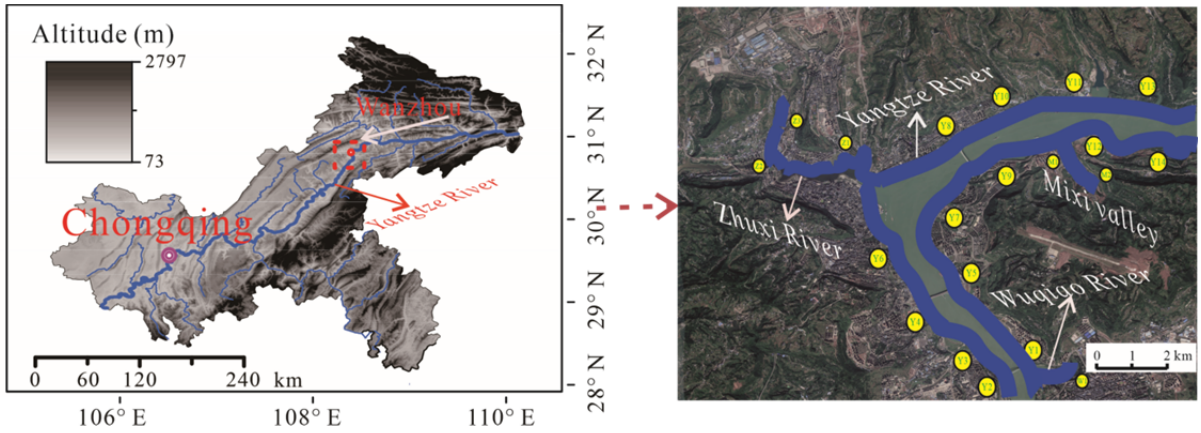

Fig. 1 Soil sample sites in the riparian zone of the Three Gorges Reservoir (TGR) in the Wanzhou section. Y1-Y14:sample points of Yangzi River; Z1-Z3:sample points of Zhuxi River; M1-M2: sample points of Mixi Valley; W1: sample point of Wuqiao River.

Table 1 Soil physicochemical properties of the riparian zone in the Wanzhou section. Values represent the means of three replicates with standard deviations behind them.

[a] Clay (%)	[a] Silt (%)	[a] Sand (%)	[b] pH	[c] WHC (%)	[d] bulk density (g·cm^{-3})
4.95±2.61	13.30±3.89	81.75±16.97	8.15±0.08	21.60±2.58	1.42±0.09
[e] TC (g·kg^{-1})	[e] TN (g·kg^{-1})	C: N ratio	[f] CEC (cmol·kg^{-1})	[g] TP (g·kg^{-1})	
12.02±0.20	1.31±0.01	9.18±0.59	19.89±2.36	0.84±4.19	

Notes: [a] hydrometer method (Ashworth et al. 2001); [b] 1:2.5 soil-water ratio by a digital pH meter in deionized water; [c] ring knife method; [d] gravimetric method (Wei et al. 2015); [e] detected by an element analyzer; [f] determined by the method of barium chloride buffer (Hendershot and Duquette 1986); [g] measured by the method of alkaline oxidation (Dick and Tabatabai 1977).

Table 2 Phosphorus fraction contents detected by the modified Hedley sequential P fractionation procedure (Maranguit et al. 2017b) in the riparian zone soil (mg·kg^{-1}). Values represent the means of three replicates with standard deviations behind them.

H_2O-Pi	$NaHCO_3$-Pi	$NaHCO_3$-Po	NaOH-Pi	NaOH-Po	HCl-Pi	Residual P
5.60±0.46	16.93±0.67	6.77±0.10	23.46±0.56	4.35±0.06	170.37±0.92	617.23±5.12

deionized water addition. Second, the samples were stabilized at ambient temperature for three days to avoid soil disturbance. Then, different concentrations of KH_2PO_4 solution were added so that P fertilizer application rates were equal to the above experimental design. Meanwhile, soil moisture content was adjusted to 60% WHC, the optimum value for microbial growth (Zhang et al. 2019). Last, soils in each bottle were thoroughly mixed for following incubations.

For the drying incubation, bottles were sealed with parafilm, and holes were left on the parafilm through acupuncture for ventilation. For the flooding incubation, deionized water (200 mL) was added to each bottle with air blown out (dissolved oxygen concentration<1 mg L^{-1}) by nitrogen gas (99.99%); subsequently, bottles were sealed with parafilm. All the samples were incubated in dark for 21 days at 20°C (the mean annual temperature of this area). Soil moisture content was maintained at 60% WHC by gravimetric method (deionized water addition) during the drying incubation.

2.3 Soil P fractionation

The modified Hedley sequential P fractionation procedure was utilized to analyze soil P fractions before and after the incubations (Maranguit et al. 2017b; Redel et al. 2008). In this method, soil P is distinguished as water-soluble P (H_2O-Pi), inorganic and organic P extracted by sodium hydrogen carbonate ($NaHCO_3$-Pi, $NaHCO_3$-Po) and sodium hydroxide (NaOH-Pi, NaOH-Po), inorganic P extracted by hydrochloric acid (HCl-Pi) and residual P. After the drying incubation, triplicate 1 g air-dried (room temperature for 5 days) soils from each sample were weighted in 50 ml plastic centrifuge tubes with screw caps. Subsequently, the soils were sequentially extracted with 30 mL deionized water, 0.5 M $NaHCO_3$, 0.1 M NaOH, and 1M HCl for the determinations of

H_2O-Pi, $NaHCO_3$-Pi ($NaHCO_3$-Po), NaOH-Pi (NaOH-Po) and HCl-Pi, respectively. Finally, residues were digested by H_2SO_4 (18M) and H_2O_2 (30%) for residual P determination. After the flooding incubation, the bottles were directly centrifugated, the supernatant was utilized for H_2O-Pi determination, and the other P fractions were detected by the method described above.

After shaking for 16 hours in a reciprocal shaker operated at 6 rpm and centrifuging at 3500 rpm for 15 minutes, the extracts or digests of each step abovementioned were filtered through filter paper (Whatman no. 42) and stored in small vials at 4°C within 24 h for inorganic P determination. The total P of filtrates extracted by sodium hydrogen carbonate and sodium hydroxide was determined after digested by ammonium-persulfate and H_2SO_4, and filtrate organic P was calculated as the difference between the total P and the inorganic P of the filtrates.

According to the recalcitrance of soil P fractions, the above-mentioned P fractions were grouped into the following pools: (1) labile P including P dissolved in soil solution (H_2O-Pi) along with loosely adsorbed P ($NaHCO_3$-Pi); (2) precipitated P including Fe (Al, Ca)-bound P (NaOH-Pi and HCl-Pi); (3) organic P including $NaHCO_3$-Po and NaOH-Po; (4) residual P comprising highly stable organometallic complexes and organic materials such as lignin (Jiménez et al. 2019; Maranguit et al. 2017b).

2.4 Chemical analyses

Soil pH was determined in a 1:2.5 soil-water ratio by a digital pH meter in deionized water. Soil TC and TN were detected by an element analyzer (EA3000, Euro Vector, Milan, Italy). Soil particle composition and WHC were measured by the hydrometer method and the ring knife method, respectively (Ashworth et al. 2001). Soil bulk density was detected by the gravimetric method (Wei et al. 2015). Total P and CEC were determined by the alkaline oxidation method (Dick and Tabatabai 1977) and the barium chloride buffer method (Hendershot and Duquette 1986), respectively. Inorganic P of filtrates and digests were detected by the method of ascorbic acid-molybdenum blue (Murphy and Riley 1962).

2.5 Statistical analysis

To clarify soil P fraction distribution as affected by applied P fertilizer, percentage changes of P fractions after the incubations were calculated as P fraction contents after the incubations minus original contents of soil P fractions divided by original contents of soil P fractions. Meanwhile, to evaluate the effect of P fertilizer application rates on P fraction distribution, transformation percentages of P fertilizer (TPPF) to soil P fractions were calculated as content differences of soil P fractions between fertilizer addition and none fertilizer addition divided by soil TP increases caused by fertilizer addition. Soil P fraction differences between the flooding and drying incubations under the same application rate of P fertilizer (ΔH_2O-Pi, $\Delta NaHCO_3$-Pi, $\Delta NaHCO_3$-Po, ΔNaOH-Pi, NaOH-Po, ΔHCl-Pi, and Δresidual P) were calculated to analyze the effect of flooding on soil P fraction transformation. Percentage change differences of soil P fractions and TPPF to soil P fractions between the drying and flooding incubations were detected by one-way ANOVA. Multivariate linear regression models were applied to detect the relationships among ΔH_2O-Pi, $\Delta NaHCO_3$-Pi, $\Delta NaHCO_3$-Po, ΔNaOH-Pi, ΔNaOH-Po, ΔHCl-Pi, and Δresidual P (Table 3). Structural equation models were used to analyze multivariate effects of P application rates on labile P via soil P fractions (Fig. 2). Potential relationships (causes) between the

Table 3 Multivariate linear regression analyses for soil P fraction differences between the drying and flooding environments.

P fractions	Equations	R^2	p
H_2O-Pi	ΔH_2O-Pi=-3.719−1.760ΔNaOH-Pi−2.443$\Delta NaHCO_3$-Po	0.927	<0.001
$NaHCO_3$-Pi	ns	ns	ns
$NaHCO_3$-Po	$\Delta NaHCO_3$-Po=-0.972+0.744ΔNaOH-Pi−0.366ΔH_2O-Pi	0.989	<0.001
NaOH-Pi	ΔNaOH-Pi=6.924−0.822ΔHCl-Pi+0.176$\Delta NaHCO_3$-Po	0.978	<0.001
NaOH-Po	ns	ns	ns
HCl-Pi	ΔHCl-Pi=2.286−0.987ΔNaOH-Pi	0.975	<0.001
Residual P	ns	ns	ns

Notes: n=30; Δ represents content differences of soil P fractions between the drying and flooding environments. ns denotes no significance.

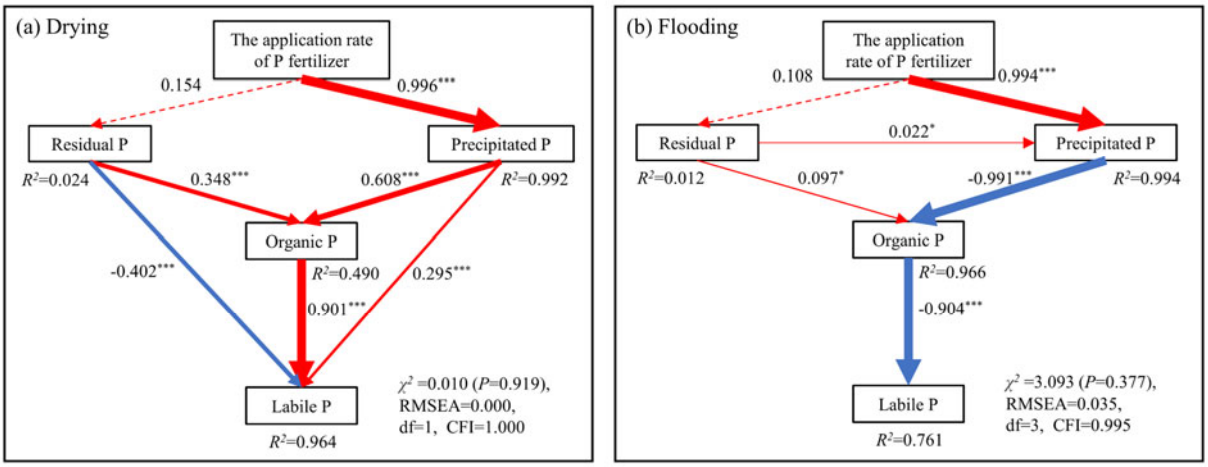

Fig. 2 Structural equation model analyses show multivariate effects of P fertilizer application rates on labile P via soil P fractions under the drying (a) and flooding (b) environments. Arrows indicate hypothesized directions of causation. The thickness of the arrows indicates the strength of the correlation between the variables. Positive and negative effects are displayed by red and blue one-way arrows. Standardized path coefficients are shown next to the arrows. Solid and dashed arrows represent significant (p < 0.05) and non-significant (p > 0.05) relationships. * and *** represent p < 0.05 and p < 0.001. Proportions of variance explained (R^2) are shown below each response variable in the models, and the results of goodness-of-fit statistics are shown alongside the models. Labile P includes H_2O-Pi and $NaHCO_3$-Pi, organic P includes $NaHCO_3$-Po and NaOH-Po and precipitated P includes NaOH-Pi and HCl-Pi; n=30.

variables in structural equation models were detected using a partial regression coefficient (direct effect), which is referred to as path coefficients (β), and indirect effects are referred to as the effects between two variables that are mediated by another intervening variable (Appendix 1). The fits of structural equation models were evaluated using the χ^2 test, the degree of freedom (df), the P-value, the root mean square error of approximation (RMSEA), and the comparative fit index (CFI) ($\chi^2(p>0.05)$, χ^2/df≤2, RMSEA≤0.06, CFI≥0.95). All the statistical analyses were performed by IBM SPSS Statistics 17 (IBM SPSS Inc.), and graphs were drawn by SigmaPlot 12.0 (Systat Software Inc.). Structural equation model analyses were performed by IBM SPSS Amos 24 (IBM Corp., 2016).

3 Results

3.1 Percentage changes of soil P fractions after incubation

Percentage changes of H_2O-Pi, NaOH-Pi, and HCl-Pi increased with P fertilizer application rates after incubation under the drying and flooding environments (Fig. 3). Percentage changes of $NaHCO_3$-Pi and NaOH-Po increased gradually with P fertilizer application rates and then remained stable under the drying and flooding environments. $NaHCO_3$-Pi remained stable at 50 kg P ha^{-1} under the drying environment and at 150 kg P ha^{-1} under the flooding environment, and NaOH-Po remained stable at 35 kg P ha^{-1} under the drying and flooding environments. $NaHCO_3$-Po increased with P fertilizer application rates under the drying environment, while an opposite trend was observed under the flooding environment.

Compare with 0 kg P ha^{-1}, as the P fertilizer rate was increased to 230 kg P ha^{-1}, H_2O-Pi, $NaHCO_3$-Pi, NaOH-Pi, NaOH-Po, and HCl-Pi were increased by 11.85 mg kg^{-1}, 18.03 mg kg^{-1}, 108.67 mg kg^{-1}, 0.40 mg kg^{-1}, and 86.30 mg kg^{-1}, respectively, under the drying environment and by 17.00 mg kg^{-1}, 22.86 mg kg^{-1}, 46.57 mg kg^{-1}, 0.48 mg kg^{-1}, and 142.57 mg kg^{-1}, under the flooding environment. In addition, $NaHCO_3$-Po was increased by 1.16 mg kg^{-1} under the drying environment and was decreased by 2.93 mg kg^{-1} under the flooding environment. Correspondingly, the percentage changes of H_2O-Pi, NaOH-Pi, HCl-Pi, $NaHCO_3$-Pi, and NaOH-Po were increased by 215.74%, 465.73%, 52.56%,116.85%, and 6.81%, respectively, under the drying environment and by 309.78%, 199.59%, 85.49%, 149.17%, and 8.50%, respectively, under the flooding environment. In addition, the percentage change of $NaHCO_3$-Po was increased by 6.15% under the drying environment and was decreased by 15.47% under the flooding environment.

The proportion of labile P in total P increased with P fertilizer application rates and then remained stable (Fig. 4). The proportion of precipitated P in total P increased with P fertilizer application rates, while residual P showed an opposite trend.

The percentage changes of H_2O-Pi and HCl-Pi under the flooding environment were higher than that under the drying environment, and opposite trends were observed for the percentage changes of $NaHCO_3$-Po and NaOH-Pi (Fig. 3, $p<0.01$). For the percentage change of $NaHCO_3$-Pi, significant differences between the drying and flooding environments were only detected below 95 kg P ha^{-1} ($p<0.05$). For the percentage changes of NaOH-Po and residual P, no significant differences were observed between the drying and flooding environments ($p>0.05$).

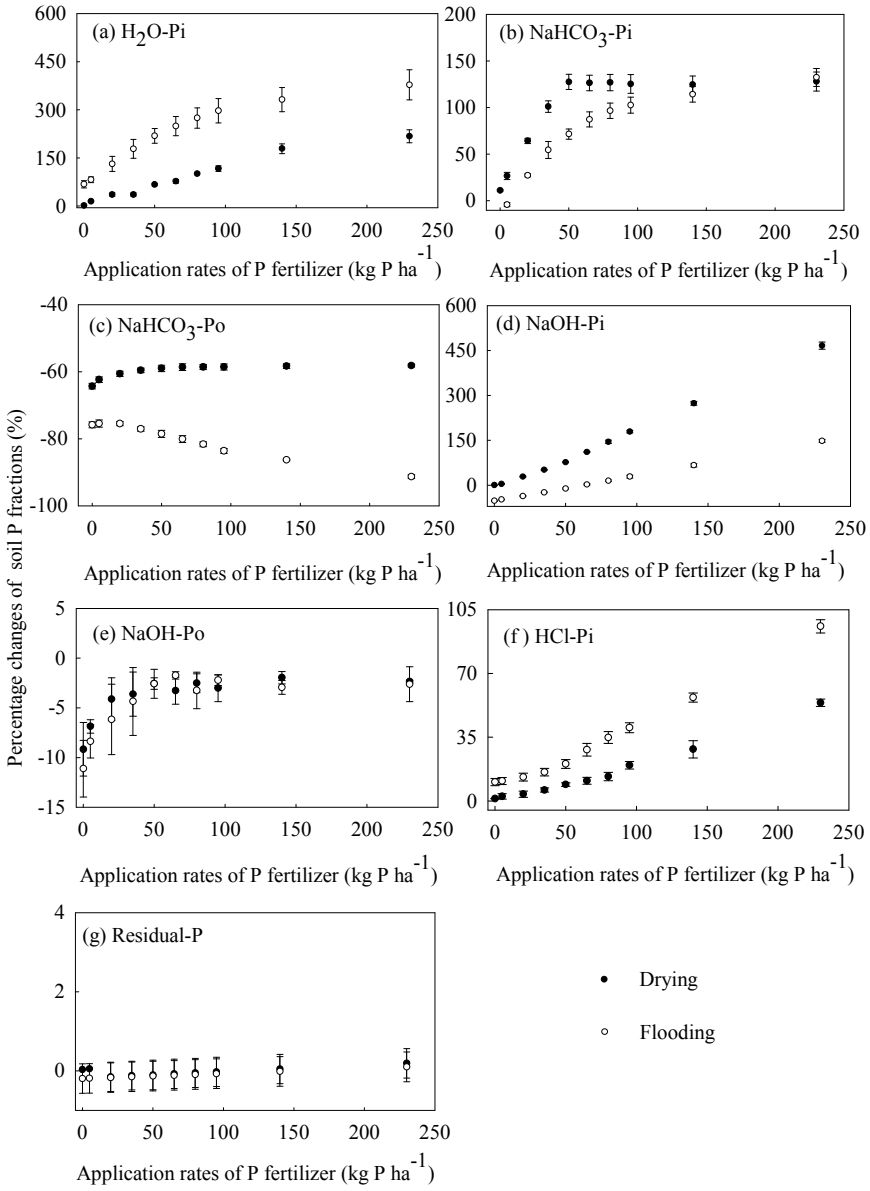

Fig. 3 Effects of P fertilizer application rates on percentage changes of soil P fractions after incubation under the drying and flooding environments. Bars represent standard deviations of means (n=3).

3.2 Transformation percentages of P fertilizer to soil P fractions

Compare with 0 kg P ha^{-1}, as the application rate of P fertilizer reached 230 kg P ha^{-1}, the transformation percentages of P fertilizer (TPPF) to H_2O-Pi, $NaHCO_3$-Pi, $NaHCO_3$-Po, and NaOH-Po were decreased by 8.91%, 25.81%, 6.89%, and 3.46%, respectively, under the drying environment and by 13.94%, 31.14%, 2.81%, and 3.82% under the flooding environment (Fig. 5). Instead, the TPPF to NaOH-Pi and HCl-Pi were increased by 20.91% and 24.26%, respectively, under the drying environment and by 9.71% and 40.72% under the flooding environment. No significant differences were observed for the TPPF to residual P among the P fertilizer application rates under the drying and flooding environments ($p>0.05$).

The TPPF to H_2O-Pi and HCl-Pi under the flooding environment was higher than that under the drying environment, and the TPPF to $NaHCO_3$-Po and NaOH-Pi showed an opposite trend ($p<0.01$). For the TPPF to $NaHCO_3$-Pi, significant differences between the drying and flooding environments were only detected below 65 kg P ha^{-1} ($p<0.05$). For the TPPF to NaOH-Po and residual P, no significant differences were observed between the drying and flooding environments

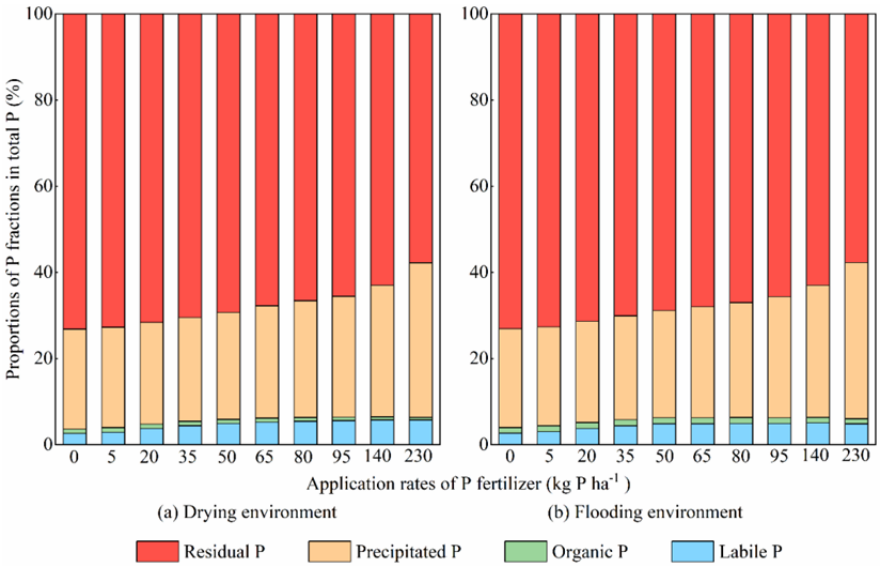

Fig. 4 Effects of P fertilizer application rates on P fraction proportions in soil total P. Labile P includes H_2O-Pi and $NaHCO_3$-Pi; Organic P includes $NaHCO_3$-Po and NaOH-Po; Precipitated P includes NaOH-Pi and HCl-Pi.

(p >0.05).

3.3 Pathways of soil P fraction transformations as affected by applied P fertilizer

Structural equation models show multivariate effects of P application rates on labile P via soil P fractions under the drying and flooding environments ($0 \le \chi 2 / df \le 2$, $0.05 < p \le 1$, RMSEA ≤ 0.06 and CFI ≥ 0.95, Fig. 2, Appendix 1). Phosphorus fertilizer application rates had direct positive effects on precipitated P with path coefficients (β) of 0.996 and 0.994 (p <0.001) under the drying and flooding environments. In addition, P fertilizer application rates had indirect positive and negative effects on organic P with β of 0.606 and -0.985 mainly via precipitated P (p <0.001) under the drying and flooding environments. Moreover, P fertilizer application rates further had indirect positive effects on labile P with β of 0.594 and 0.883 via organic P (p <0.001) under the drying and flooding environments. Phosphorus fertilizer application rates also had a further indirect positive effect on labile P with β of 0.294 via precipitated P (p <0.001) under the drying environment. Residual P had direct positive effects on organic P under the drying and flooding environments (p <0.05). Organic P had direct positive and negative effects on labile P under the drying and flooding environments (p <0.001). Residual P had a direct negative effect on labile P under the drying environment (p <0.001). Organic P, residual P, and precipitated P explained 96.4% of the total variance in labile P under the drying environment. Organic P explained 76.1% of the total variance in labile P under the flooding environment. Residual P had a direct positive effect on precipitated P under the flooding environment (p <0.001). Precipitated P had a positive (negative) effect on organic P, and organic P had a positive (negative) effect on labile P under the drying (flooding) environment.

3.4 Relationships among soil P fraction differences between the drying and flooding environments

Multivariate linear regression analyses were performed on soil P fraction differences between the flooding and drying environments (Table 3). Δ H_2O-Pi was negatively correlated with ΔNaOH-Pi and $\Delta NaHCO_3$-Po (p <0.001). $\Delta NaHCO_3$-Po was positively correlated with ΔNaOH-Pi, and ΔNaOH-Pi was negatively correlated with ΔHCl-Pi (p <0.001).

4 Discussion

4.1 Soil P fraction distributions affected by applied P fertilizer

The percentage change of H_2O-Pi increased with P fertilizer application rates, and the percentage change of $NaHCO_3$-Pi increased with P fertilizer application rates and then remained stable under the

drying and flooding environments (Fig. 3). Gradual transformation of precipitated P into labile P by microorganisms could be responsible for the results (Wang et al. 2022; Brucker et al. 2020; Pastore et al. 2020), supported by the indirect effects of P fertilizer application rates on labile P via precipitated P in the structural equation models (Fig. 2). Phosphorus fertilizer application increases labile P content of paddy soil and alkaline sandy loam soil (Chen et al. 2022b; Cao et al. 2022), which are consistent with our results.

The percentage changes of NaOH-Pi and HCl-Pi increased with P fertilizer application rates (Fig. 3), which is consistent with our first hypothesis. Alkaline soil environment (pH = 8.15, Table 1) with high contents of Ca, Al, and Fe ions (we did not measure contents of Ca carbonate and Al/Fe (hydro)oxides in the tested soil, but Li et al. (2007) did) could be the reason for the results. The results indicated that inorganic P input increased soil P release risk (especially for Fe-bound P) from the riparian zone to the TGR under rain-leaching and flooding environments. The increases of NaOH-Pi and HCl-Pi were also observed in black soil, fluvo-aquic soil, and red soil under the drying environment (Luo et al. 2017). Calcium-bound P is the main fraction increased by P fertilizer application in submerged calcareous soil rather than Fe-bound P (Abolfazli et al. 2012), which partly agrees with our results. Compare with calcareous soil, the high content of Al (Fe) oxides/hydroxides in the purple alluvial soil measured by Li et al.(2007) as mentioned above could be the reason for simultaneous large increases of $NaHCO_3$-Pi and NaOH-Pi in our study. Manure application decreases Ca-bound P in calcareous soil

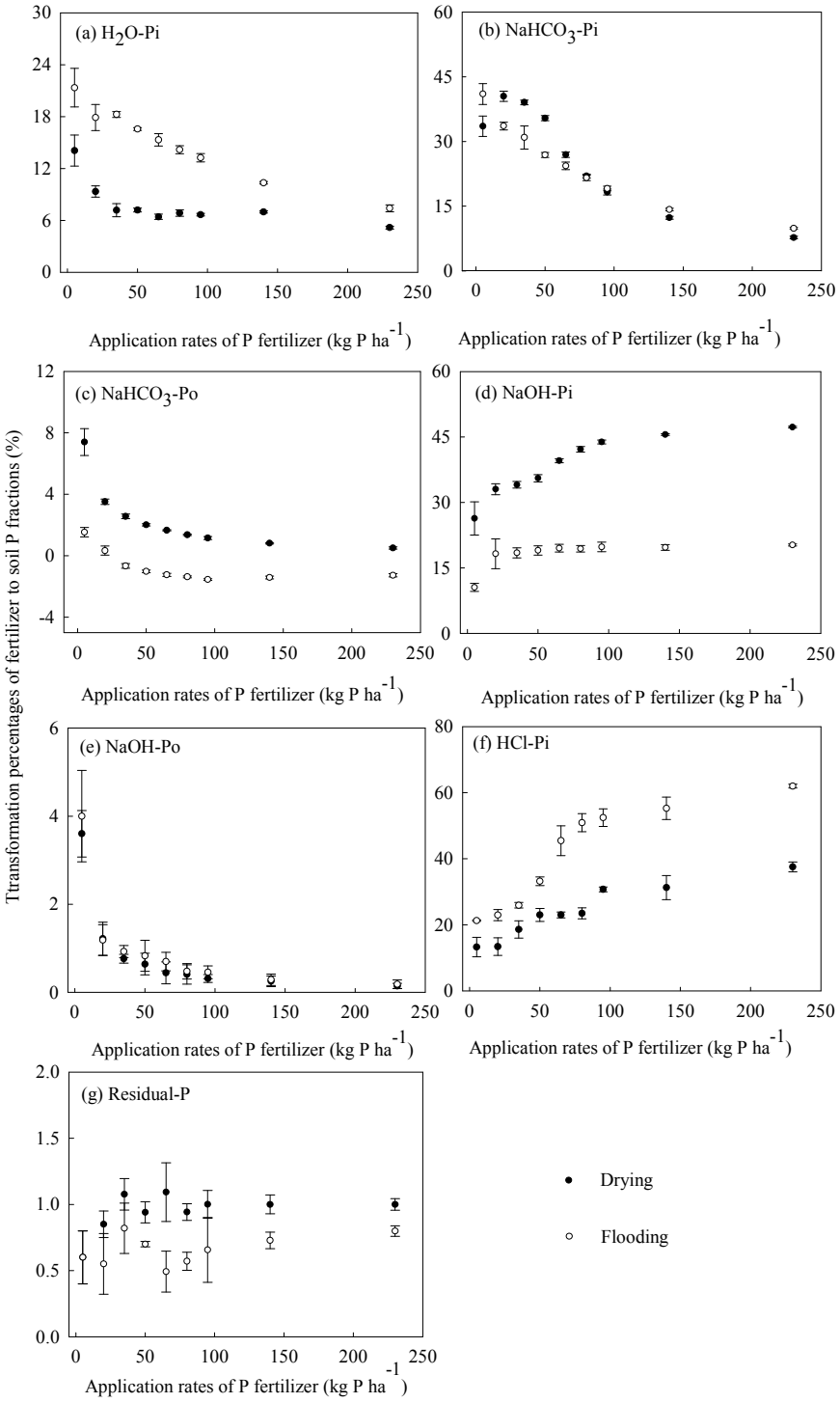

Fig. 5 Effects of P fertilizer application rates on transformation percentages of P fertilizer to soil P fractions under the drying and flooding environments. Bars represent standard deviations of the means (n=3).

(Yan et al. 2018), which is opposite to our result. Soil pH decrease caused by manure application should be the reason for this controversy (Yan et al. 2018). Hence, the effect of organic P fertilizer application on soil P fraction distribution in the riparian zone should be further investigated in the future. Residual P and NaOH-Pi are the main fractions presenting in paddy soil after 40 years of continuous fertilization (Yan et al. 2017), which is consistent with our result of NaOH-Pi but disagrees with the result of residual P. Our study is a short-term incubation experiment with only one fertilization, whereas the above study is a long-term experiment with intermittent fertilization. In addition, long-term microbial processes could result in residual P increase (Audette et al. 2016). Therefore, differences in experiment duration and fertilization frequency may be the main reasons for this inconsistency, which needs to be explored in the future.

In the drying environment, $NaHCO_3$-Po increased with P fertilizer application rates, while an opposite trend was observed in the flooding environment (Fig. 3). Precipitated P transformation to organic P by microorganisms (Menezes-Blackburn et al. 2016; Tian et al. 2021) could be responsible for the result in the drying environment, supported by the direct positive effect of precipitated P on organic P in the structural equation model (Fig. 2). Organic P release caused by Fe-bound P reduction (Bai et al. 2020; Maranguit et al. 2017a) could be the reason for the result in the flooding environment, supported by the direct negative effect of precipitated P on organic P in the structural equation model (Fig. 2). NaOH-Po initially increased with P fertilizer application rates and finally kept stable under the drying and flooding environments (Fig. 3). Since chemically bonded P is more stable than physically adsorbed P, we presume that NaOH-Po is chemically bonded organic P, needing further investigation. Inorganic P fertilizer application leads to soil organic P accumulation in the organic layer of a forest ecosystem (Spohn et al. 2018), which is consistent with our result. Long-term organic fertilizer application has little effect on soil organic P in the topsoil of a slightly acidic luvisol under the drying environment (Annaheim et al. 2015), and animal manure input increases organic P content in paddy soil under the flooding environment (Chen et al. 2022b). Both of the results of the above studies disagree with our results. The effect of organic fertilizer input on soil pH is different due to soil type differences, affecting microbial P assimilation processes (Dai et al. 2020; Kong et al. 2018; Audette et al. 2016; Soltangheisi et al. 2018). Therefore, the differences in P fertilizer and soil types could be the reason for the controversy.

The results of TPPF to P fractions showed that P fertilizer transformed more into precipitated P than to labile P and organic P with the increase of P fertilizer application rate under the drying and flooding environments (Fig. 5), agreeing with our first hypothesis. The high content of Al (Fe) oxides/hydroxides and Ca carbonate tested by Li et al.(2007) in the purple alluvial soil could be the reason for the results. Our results indicated that the increase of inorganic P fertilizer input increased soil P release risk (such as Fe-bound P) from the riparian zone to the TGR under the environment of alternating drying and flooding. Measures, such as prohibiting agricultural activities during the drying period and building ecological barriers between the riparian zone and agricultural fields, should be taken to control exogenous P input for the reduction of soil P release risk from the riparian zone to the TGR.

An application rate increase of inorganic P fertilizer significantly increases soil organic P content under the drying environment (Mahmood et al. 2020), which is consistent with our result. The increase of P fertilizer application rate (a mixture of organic and inorganic P fertilizer) increases labile P content and decreases Ca-bound P content in calcareous sandy loam soil under the drying environment (Ahmad et al. 2018), which is consistent with our result of labile P but opposite to the result of HCl-Pi. Soil pH decrease triggered by organic P fertilizer input could be responsible for the inconsistency (Ahmad et al. 2018). It has also been reported that both labile P and Ca-bound P are increased by the increase in manure application rate in a calcareous soil under the drying environment (Weyers et al. 2016), which is consistent with our results. The unconformity in Ca-bound P change caused by the addition of organic P fertilizer in the above studies may be related to buffering property discrepancy of different soil types (Ahmad et al. 2018), which needs to be further investigated. High application rates of inorganic P fertilizer led to labile P content increase under the drying environment in an *in situ* study, while no significant differences in labile P content were observed among low application rates of P fertilizer (Coelho et al. 2021), which only agrees with our result at high application rates. Plant

P uptake in the *in situ* study may be the reason for the discrepancy, indicating that *in situ* study should be conducted in the future. Soil characteristics of P fraction distribution affected by P fertilizer application are still unclear in the riparian zone. The results deepen our understanding of soil P fraction distribution as affected by applied P fertilizer and provide help to assess soil P release from the riparian zone to the TGR.

4.2 Soil P fraction transformation processes affected by applied P fertilizer

Under the drying environment, P fertilizer application rates had a direct positive effect on precipitated P, further mainly had an indirect positive effect on organic P via precipitated P, and finally mainly had an indirect positive effect on labile P via organic P (Fig. 2, p <0.001). The results showed that P fertilizer was first transformed into precipitated P, and then further transformed into organic P and labile P, which is consistent with our second hypothesis. The results could be explained by chemical precipitation processes of inorganic P fertilizer and further microbial transformation of precipitated P. Phosphorus fertilizer input promoted precipitated P formation, supported by the increases of NaOH-Pi and HCl-Pi with P fertilizer application rates (Figs. 3 and 4). Subsequently, phosphate-solubilizing microorganisms can dissolve the precipitated P (Han et al. 2022; Zhang et al. 2021), and the dissolved P could be transformed into organic P through microbial assimilation (Dai et al. 2020; Gross et al. 2020), supported by the increases of $NaHCO_3$-Po and NaOH-Po with P fertilizer application rates under the drying environment (Fig. 3). Further, the organic P could be mineralized to labile P, supported by the increases of $NaHCO_3$-Pi and H_2O-Pi with P fertilizer application rates (Figs. 3 and 4).

Inorganic P fertilizer is finally transformed into labile P, precipitated P, and organic P under the drying environment (Ahmad et al. 2018; Luo et al. 2017), which is consistent with our results. An 18-week incubation experiment found that labile P and moderately labile P are transformed into more stable P fractions under P fertilizer application (Audette et al. 2016), which disagrees with our results. The incubation time difference may be the reason for this discrepancy (Audette et al. 2016), which needs to be discussed in the future. With the increase of P fertilizer application rates, labile P originates from organic P mineralization in soil lacking organic matter (Jiménez et al. 2019), and P fertilizer application promotes the transformation of precipitated P to labile P in agricultural soils (Liao et al. 2021), both of which are consistent with our results. We further pointed out that organic P could be the intermediate link in the transformation processes from precipitated P to labile P in riparian zone soil.

Under the flooding environment, P fertilizer application rates had a direct positive effect on precipitated P, mainly had an indirect negative effect on organic P via precipitated P, and finally had an indirect negative effect on labile P via organic P (Fig. 2, p <0.001). The results show that P fertilizer was first transformed into precipitated P, and the precipitated P increase led to the organic P decrease and the labile P increase under the flooding environment. The results are consistent with our second hypothesis in terms of the transformation of P fertilizer to precipitated P but disagree in terms of the further transformations from precipitated P to organic P and labile P. Chemical precipitation could be still responsible for the direct positive effect of P fertilizer application rate on precipitated P as interpreted above. $NaHCO_3$-Po desorption caused by Fe-bound P reduction release under the flooding environment (Bai et al. 2020; Maranguit et al. 2017a) could be the reason for the inconsistent results, supported by the lower contents of NaOH-Pi and $NaHCO_3$-Po under the flooding environment than that under the drying environment (Fig. 3), positive correlation between ΔNaOH-Pi and $\Delta NaHCO_3$-Po and negative correlation between ΔH_2O-Pi and $\Delta NaHCO_3$-Po (Table 3, p <0.001). The effect of P fertilizer input on the transformation processes of soil P fraction is still unclear under the flooding environment. Our results point out that labile P originated from organic P release caused by precipitated P dissolution under the flooding environment. The results deepen our understanding of the transformation processes of soil P fraction affected by inorganic P fertilizer application under the drying and flooding environments and could provide a scientific basis for preventing and controlling soil P release from the riparian zone.

4.3 Effect of flooding on soil P fraction distribution

Negative linear relationships between ΔH_2O-Pi and $\Delta NaHCO_3$-Po and between ΔHCl-Pi and ΔNaOH-Pi were observed (Table 3, p <0.001). The results indicated that H_2O-Pi release came from $NaHCO_3$-Po mineralization, and the HCl-Pi increase was caused by further precipitation of NaOH-Pi release under the flooding environment, which is consistent with our third hypothesis. $NaHCO_3$-Po and NaOH-Pi release caused by microbial reduction dissolution of Fe-bound P under the flooding environment (Maranguit et al. 2017a) could be the reason for the results. This explanation was supported by higher percentage changes of $NaHCO_3$-Po and NaOH-Pi and TPPF to $NaHCO_3$-Po and NaOH-Pi under the drying environment than that under the flooding environment (Fig. 3, Fig. 5, p <0.01). Since the alkaline soil environment (pH=8.15, Table 1) and high content of Ca ions in the purple alluvial soil tested by Li et al. (2007), the released NaOH-Pi could be further precipitated with calcium ions to form HCl-Pi. Flooding leads to a P availability increase and a Fe-related P decrease in wetland soil (Maranguit et al. 2017a; Kinsman-Costello et al. 2014; Bai et al. 2020), which is consistent with our results of NaOH-Pi and H_2O-Pi. However, HCl-Pi increase was not observed under the flooding environment in these studies. Differences in fertilizer application (no P fertilizer input in the above studies) and soil pH (soil environment is acidic in the above studies but is alkaline in our study (pH=8.15, Table 1)) could be responsible for this discrepancy.

Generally, it is believed that soil P release mainly comes from NaOH-Pi release caused by flooding (Gu et al. 2019; Maranguit et al. 2017a). We further reveal that, with P fertilizer application, $NaHCO_3$-Po release due to Fe-bound P reduction was the final source of P release caused by flooding. The results deepen our understanding of soil P release processes and can provide help for preventing and controlling soil P release caused by flooding.

5 Conclusions

Inorganic P fertilizer is mainly transformed into labile P (i.e., H_2O-Pi, $NaHCO_3$-Pi) and precipitated P (i.e., NaOH-Pi, HCl-Pi) in the purple alluvial soil of the riparian zone of the Three Gorges Reservoir under the drying and flooding environments. Meanwhile, except for $NaHCO_3$-Po release under the flooding environment, inorganic P fertilizer is also transformed into organic P (i.e., $NaHCO_3$-Po, NaOH-Po) by microbial assimilation. With the application rate increase of P fertilizer, inorganic P fertilizer is transformed more into precipitated P than into labile P and organic P. Inorganic P fertilizer mainly increases organic P via precipitated P under the drying environment and decreases organic P via precipitated P under the flooding environment. Finally, the organic P is transformed into labile P. With P fertilizer input, P release caused by flooding is derived from $NaHCO_3$-Po release triggered by the reductive release of NaOH-Pi. The results is helpful for the understanding of soil migration processes of inorganic P fertilizer from the riparian zone to the Three Gorges Reservoir under rain leaching and flooding and can provide scientific reference for the prevention and control of soil P release from the riparian zone. There are also shortcomings in our study. Phosphorus fertilizer transformation processes should be investigated under periodic drying and flooding hydrological environments. In addition, the chemical and microbial transformation mechanisms of P fertilizer should be further discussed. Moreover, it should be concerned with the effects of different kinds of P fertilizer, application frequencies of P fertilizer, plant uptake, and incubation time extension on the distribution and transformation of soil P fraction.

Acknowledgments

This work was supported by the Program of Chongqing Science and Technology Commission (cstc2020jcyj-msxmX0095); the Chongqing Municipal Key Laboratory of Institutions of Higher Education (WEPKL2018ZD-05); the Science and Technology Research Program of Chongqing Municipal Education Commission (KJZD-K202001203, KJZD-K202003501); the Innovative Research Group of Universities in Chongqing (CXQT P19037); the Sustainable Development Research Centre of Three Gorges Reservoir Area (18sxxyjd11).

Electronic supplementary material: Supplementary material (Appendix 1) is available in the online version of this article at https://doi.org/10.1007/s11629-022-7707-9

References

Abolfazli F, Forghani A, Norouzi M (2012) Effects of phosphorus and organic fertilizers on phosphorus fractions in submerged soil. J Soil Sci Plant Nut 12(2): 349-362. https://doi.org/10.4067/S0718-95162012000200014

Ahmad M, Ahmad M, El-Naggar AH, et al. (2018) Aging effects of organic and inorganic fertilizers on phosphorus fractionation in calcareous sandy loam soil. Pedosphere 28(6): 873-883. https://doi.org/10.1016/s1002-0160(17)60363-1

Ahmed W, Jing H, Kaillou L, et al. (2019) Changes in phosphorus fractions associated with soil chemical properties under long-term organic and inorganic fertilization in paddy soils of southern China. PloS One 14(5): e0216881. https://doi.org/10.1371/journal.pone.0216881

Annaheim KE, Doolette AL, Smernik RJ, et al. (2015) Long-term addition of organic fertilizers has little effect on soil organic phosphorus as characterized by ^{31}P NMR spectroscopy and enzyme additions. Geoderma 257: 67-77. https://doi.org/10.1016/j.geoderma.2015.01.014

Ashworth J, Keyes D, Kirk R, et al. (2001) Standard procedure in the hydrometer method for particle size analysis. Commun Soil Sci Plan 32(5-6): 633-642. https://doi.org/10.1081/CSS-100103897

Audette Y, O'Halloran IP, Voroney RP (2016) Kinetics of phosphorus forms applied as inorganic and organic amendments to a calcareous soil. Geoderma 262: 119-124. https://doi.org/10.1016/j.geoderma.2015.08.021

Bai J, Yu L, Ye X, et al. (2020) Dynamics of phosphorus fractions in surface soils of different flooding wetlands before and after flow-sediment regulation in the Yellow River estuary, China. J Hydrol 580: 124256. https://doi.org/10.1016/j.jhydrol.2019.124256

Bao Y, Gao P, He X (2015) The water-level fluctuation zone of Three Gorges Reservoir—A unique geomorphological unit. Earth-Sci Rev 150: 14-24. https://doi.org/10.1016/j.earscirev.2015.07.005

Brucker E, Kernchen S, Spohn M (2020) Release of phosphorus and silicon from minerals by soil microorganisms depends on the availability of organic carbon. Soil Biol Biochem 143:107737. https://doi.org/10.1016/j.soilbio.2020.107737

Cao N, Zhi M, Zhao W, et al. (2022) Straw retention combined with phosphorus fertilizer promotes soil phosphorus availability by enhancing soil P-related enzymes and the abundance of phoC and phoD genes. Soil Till Res 220: 105390. https://doi.org/10.1016/j.still.2022.105390

Chen X, Yan X, Wang M, et al. (2022a) Long-term excessive phosphorus fertilization alters soil phosphorus fractions in the acidic soil of pomelo orchards. Soil Till Res 215: 105214. https://doi.org/10.1016/j.still.2021.105214

Chen G, Yuan J, Chen H, et al. (2022b) Animal manures promoted soil phosphorus transformation via affecting soil microbial community in paddy soil. Sci Total Environ 831:154917. https://doi.org/10.1016/j.scitotenv.2022.154917

Chen X, Zhang S, Liu D, et al. (2019) Nutrient inputs from the leaf decay of Cynodon dactylon (L.) Pers in the water level fluctuation zone of a Three Gorges tributary. Sci Total Environ 688: 718-723. https://doi.org/10.1016/j.scitotenv.2019.06.357

Chen Z, Fang F, Shao Y, et al. (2021) The biotransformation of soil phosphorus in the water level fluctuation zone could increase eutrophication in reservoirs. Sci Total Environ 763: 142976. https://doi.org/10.1016/j.scitotenv.2020.142976

Coelho MJA, Ruiz-Diaz D, Rodrigues M, et al. (2021) Soil phosphorus fate and its lability after a long-term phosphorus fertilizer strategy in Brazilian Oxisol. Arch Agron Soil Sci 67(12): 1694-1707. https://doi.org/10.1080/03650340.2020.1803492

Dai Z, Liu G, Chen H, et al. (2020) Long-term nutrient inputs shift soil microbial functional profiles of phosphorus cycling in diverse agroecosystems. ISME J 14(3): 757-770. https://doi.org/10.1038/s41396-019-0567-9

Dick W, Tabatabai M (1977) An alkaline oxidation method for determination of total phosphorus in soils. Soil Sci Soc Am J 41(3): 511-514. https://doi.org/10.2136/sssaj1977.03615995004100030015x

Fu D, Xu Z, Wu X, et al. (2021) Land use effects on soil phosphorus behavior characteristics in the eutrophic aquatic-terrestrial ecotone of Dianchi Lake, China. Soil Till Res 205: 104793. https://doi.org/10.1016/j.still.2020.104793

Gross A, Lin Y, Weber PK, et al. (2020) The role of soil redox conditions in microbial phosphorus cycling in humid tropical forests. Ecology 101(2): e02928. https://doi.org/10.1002/ecy.2928

Gu C, Margenot AJ (2021) Navigating limitations and opportunities of soil phosphorus fractionation. Plant Soil 459(1): 13-17. https://doi.org/10.1007/s11104-020-04552-x

Han L, Wang X, Li B, et al. (2022) Enhanced Fe-bound phosphate availability by the combined use of Mg-modified biochar and phosphate-solubilizing bacteria. J Environ Chem Eng 10(2): 107232. https://doi.org/10.1016/j.jece.2022.107232

Hendershot WH, Duquette M (1986) A simple barium chloride method for determining cation exchange capacity and exchangeable cations. Soil Sci Soc Am J 50(3): 605-608. https://doi.org/10.2136/sssaj1986.03615995005000030013x

Huang LM, Thompson A, Zhang GL (2014) Long-term paddy cultivation significantly alters topsoil phosphorus transformation and degrades phosphorus sorption capacity. Soil Till Res 142: 32-41. https://doi.org/10.1016/j.still.2014.04.007

Jiménez JL, Healy MG, Daly K (2019) Effects of fertilizer on phosphorus pools in soils with contrasting organic matter content: A fractionation and path analysis study. Geoderma 338:128-135. https://doi.org/10.1016/j.geoderma.2018.11.049

Joshi SR, Li X, Jaisi DP (2016) Transformation of phosphorus pools in an agricultural soil: An application of oxygen - 18 labeling in phosphate. Soil Sci Soc Am J 80(1): 69-78. https://doi.org/10.2136/sssaj2015.06.0219

Kinsman-Costello LE, O'Brien J, Hamilton SK (2014) Re-flooding a historically drained wetland leads to rapid sediment phosphorus release. Ecosystems 17(4): 641-656. https://doi.org/10.1007/s10021-014-9748-6

Kong Y, Zhu C, Ruan Y, et al. (2018) Are the microbial communities involved in glucose assimilation in paddy soils treated with different fertilization regimes for three years similar? J Soil Sediment 18: 2476-2490. https://doi.org/10.1007/s11368-018-1961-z

Li M, Hou Y, Zhu B (2007) Phosphorus sorption-desorption by purple soils of China in relation to their properties. Soil Res 45(3): 182-189. https://doi.org/10.1071/SR06135

Liao D, Zhang C, Lambers H, et al. (2021) Changes in soil phosphorus fractions in response to long-term phosphate fertilization under sole cropping and intercropping of maize and faba bean on a calcareous soil. Plant Soil 463(1): 589-600. https://doi.org/10.1007/s11104-021-04915-y

Luo L, Ma Y, Sanders RL, et al. (2017) Phosphorus speciation and transformation in long-term fertilized soil: evidence from chemical fractionation and P K-edge XANES spectroscopy. Nutr Cycl Agroecosys 107(2): 215-226. https://doi.org/10.1007/s10705-017-9830-5

Mahmood M, Tian Y, Ma Q, et al. (2020) Changes in phosphorus fractions and its availability status in relation to long term phosphorus fertilization in loess plateau of China. Agronomy 10(11): 1818. https://doi.org/10.3390/agronomy10111818
Maranguit D, Guillaume T, Kuzyakov Y (2017a) Effects of flooding on phosphorus and iron mobilization in highly weathered soils under different land-use types: Short-term effects and mechanisms. Catena 158: 161-170. https://doi.org/10.1016/j.catena.2017.06.023
Maranguit D, Guillaume T, Kuzyakov Y (2017b) Land-use change affects phosphorus fractions in highly weathered tropical soils. Catena 149: 385-393. https://doi.org/10.1016/j.catena.2016.10.010
Meena MD, Narjary B, Sheoran P, et al. (2018) Changes of phosphorus fractions in saline soil amended with municipal solid waste compost and mineral fertilizers in a mustard-pearl millet cropping system. Catena 160: 32-40. https://doi.org/10.1016/j.catena.2017.09.002
Menezes-Blackburn D, Paredes C, Zhang H, et al. (2016) Organic acids regulation of chemical–microbial phosphorus transformations in soils. Environ Sci Technol 50(21): 11521-11531. https://doi.org/10.1021/acs.est.6b03017
Mitran T, Mani PK, Basak N, et al. (2016) Long-term manuring and fertilization influence soil inorganic phosphorus transformation vis-a-vis rice yield in a rice-wheat cropping system. Arch Agron Soil Sci, 2016, 62(1): 1-18. https://doi.org/10.1080/03650340.2015.1036747
Murphy J, Riley JP (1962) A modified single solution method for the determination of phosphate in natural waters. Anal. Chim. Acta, 27(C), 678-681. https://doi.org/10.1016/S0003-2670(00)88444-5
Pastore G, Kaiser K, Kernchen S, et al. (2020) Microbial release of apatite-and goethite-bound phosphate in acidic forest soils. Geoderma 370: 114360. https://doi.org/10.1016/j.geoderma.2020.114360
Redel Y, Rubio R, Godoy R, et al. (2008) Phosphorus fractions and phosphatase activity in an Andisol under different forest ecosystems. Geoderma 145(3-4): 216-221. https://doi.org/10.1016/j.geoderma.2008.03.007
Saia SM, Carrick HJ, Buda AR, et al. (2021) Critical review of polyphosphate and polyphosphate accumulating organisms for agricultural water quality management. Environ Sci Technol 55(5): 2722-2742. https://doi.org/10.1021/acs.est.0c03566
Soltangheisi A, Rodrigues M, Coelho MJA, et al. (2018) Changes in soil phosphorus lability promoted by phosphate sources and cover crops. Soil Till Res 179: 20-28. https://doi.org/10.1016/j.still.2018.01.006
Spohn M, Zavišić A, Nassal P, et al. (2018) Temporal variations of phosphorus uptake by soil microbial biomass and young beech trees in two forest soils with contrasting phosphorus stocks. Soil Biol Biochem 117: 191-202. https://doi.org/10.1016/j.soilbio.2017.10.019
Tian J, Ge F, Zhang D, et al. (2021) Roles of phosphate solubilizing microorganisms from managing soil phosphorus deficiency to mediating biogeochemical P cycle. Biology 10(2): 158. https://doi.org/10.3390/biology10020158
Wang C, Guo J, Zhang W, et al. (2021) Drying-rewetting changes soil phosphorus status and enzymatically hydrolysable organic phosphorus fractions in the water-level fluctuation zone of Three Gorges reservoir. Catena 204: 105416. https://doi.org/10.1016/j.catena.2021.105416
Wang C, Thielemann L, Dippold MA, et al. (2022) Can the reductive dissolution of ferric iron in paddy soils compensate phosphorus limitation of rice plants and microorganisms? Soil Biol Biochem 168: 108653. https://doi.org/10.1016/j.soilbio.2022.108653
Wang T, Zhu B, Zhou M, et al. (2020) Nutrient loss from slope cropland to water in the riparian zone of the Three Gorges Reservoir: Process, pathway, and flux. Agr Ecosyst Environ 302: 107108. https://doi.org/10.1016/j.agee.2020.107108
Wei Y, Wu X, Cai C. (2015) Splash erosion of clay–sand mixtures and its relationship with soil physical properties: The effects of particle size distribution on soil structure. Catena 135: 254-262. https://doi.org/10.1016/j.catena.2015.08.003
Weyers E, Strawn DG, Peak D, et al. (2016) Phosphorus speciation in calcareous soils following annual dairy manure amendments. Soil Sci Soc Am J 80(6):1531. https://doi.org/10.2136/sssaj2016.09.0280
Xiang R, Wang L, Li H, et al. (2021) Water quality variation in tributaries of the Three Gorges Reservoir from 2000 to 2015. Water Res 195: 116993. https://doi.org/10.1016/j.watres.2021.116993
Yan X, Wei Z, Hong Q, et al. (2017) Phosphorus fractions and sorption characteristics in a subtropical paddy soil as influenced by fertilizer sources. Geoderma 295: 80-85. https://doi.org/10.1016/j.geoderma.2017.02.012
Yan Z, Chen S, Dari B, et al. (2018) Phosphorus transformation response to soil properties changes induced by manure application in a calcareous soil. Geoderma 322: 163-171. https://doi.org/10.1016/j.geoderma.2018.02.035
Ye C, Chen C, Butler OM, et al. (2019) Spatial and temporal dynamics of nutrients in riparian soils after nine years of operation of the Three Gorges Reservoir, China. Sci Total Environ 664: 841-850. https://doi.org/10.1016/j.agee.2020.107108
Zhang S, Zheng Q, Noll L, et al. (2019) Environmental effects on soil microbial nitrogen use efficiency are controlled by allocation of organic nitrogen to microbial growth and regulate gross N mineralization. Soil Biol Biochem 135: 304-315. https://doi.org/10.1016/j.soilbio.2019.05.019
Zhang Y, Li Y, Wang S, et al. (2021b) Soil phosphorus fractionation and its association with soil phosphate-solubilizing bacteria in a chronosequence of vegetation restoration. Ecol Eng 164(3): 106208. https://doi.org/10.1016/j.ecoleng.2021.106208
Zhang Z, Hu H, Wan C, et al. (2018) Lateral and longitudinal variation in phosphorus fractions in surface sediment and adjacent riparian soil in the Three Gorges Reservoir, China. Environ Sci Pollut R 25(31): 31262-31271. https://doi.org/10.1007/s11356-018-3087-7
Zhu B, Wang Z, Zhang X (2012) Phosphorus fractions and release potential of ditch sediments from different land uses in a small catchment of the upper Yangtze River. J Soil Sediment 12(2): 278-290. https://doi.org/10.1007/s11368-011-0449-x